

# Real-Time Transmission of Uncompressed High-Definition Video Via A VCSEL-Based Optical Wireless Link With Ultra-Low Latency

Hossein Kazemi, Isaac N. O. Osahon, Tiankuo Jiao, David Butler, Nikolay Ledentsov Jr., Ilya Titkov, Nikolay Ledentsov, and Harald Haas

**Abstract**—Real-time transmission of high-resolution video signals in an uncompressed and unencrypted format requires an ultra-reliable and low-latency communications (URLLC) medium with high bandwidth to maintain the quality of experience (QoE) for users. We put forward the design and experimental demonstration of a high-performance laser-based optical wireless communication (OWC) system that enables high-definition (HD) video transmission with submillisecond latencies. The serial digital interface (SDI) output of a camera is used to transmit the live video stream over an optical wireless link by directly modulating the SDI signal on the intensity of a 940 nm vertical cavity surface emitting laser (VCSEL). The proposed SDI over light fidelity (LiFi) system corroborates error-free transmission of full HD (FHD) and 4K ultra-high-definition (UHD) resolutions at data rates of 2.97 Gb/s and 5.94 Gb/s, respectively, with a measured end-to-end latency of under 35 ns. Since SDI standards support various video formats and VCSELs are high-bandwidth and low-power devices, this presents a scalable and inexpensive solution for wireless connectivity between professional broadcast equipment using off-the-shelf SDI components.

**Index Terms**—Next-generation light fidelity (LiFi), laser-based optical wireless communication (OWC), ultra-reliable low-latency communications (URLLC), serial digital interface (SDI), vertical cavity surface emitting laser (VCSEL).

## I. INTRODUCTION

Real-time and low-latency communications are among the key performance indicators for sixth generation (6G) networks to enable mission-critical applications, including autonomous systems, remote surgery, and industrial automation [1]. Hence, 6G aims to significantly advance ultra-reliable and low-latency communications (URLLC) to meet stringent requirements for reliability and responsiveness, targeting near-zero packet loss and submillisecond latencies [2]. Emerging applications such as multi-sensory extended reality (XR) technologies, including augmented reality (AR), virtual reality (VR), and mixed reality (MR), primarily rely on URLLC to ensure seamless real-time user experiences through immersive high-fidelity interactions without causing motion sickness, lag, or disorientation [2].

A key application of URLLC is live television (TV) broadcasting, where minimal latency and high reliability are crucial to guarantee real-time content delivery and uninterrupted viewer experience. British broadcasting corporation (BBC) has recently launched a low-latency streaming trial on BBC

iPlayer, aiming to reduce the delay between live broadcasts and online streaming. The trial evaluates low-latency dynamic adaptive streaming over the hypertext transfer protocol (HTTP) with the objective of bringing streaming delays closer to broadcast levels while maintaining high quality of experience (QoE) for viewers [3]. There are various digital video interfaces for the reliable transmission of high-quality multimedia content over cable connections, including high-definition multimedia interface (HDMI), DisplayPort (DP), Internet protocol (IP)-based interfaces such as network device interface (NDI), and serial digital interface (SDI) [4]. While HDMI and DP dominate consumer electronics and desktop video delivery applications, NDI, which runs over Gigabit Ethernet, is mainly adopted in information technology (IT) systems [4]. Among these interfaces, SDI remains the preferred choice in traditional broadcast infrastructures due to its robustness, low latency, and ability to support long distance transmission over coaxial or fiber-optic cables [4]. In fact, SDI is a family of digital video interfaces that was first standardized in 1989 by the Society of Motion Picture and Television Engineers (SMPTE) to transmit uncompressed, unencrypted digital video signals in broadcast TV studios and post-production facilities [4]. Existing SMPTE SDI standards support a wide range of video formats and bit rates from standard definition (SD) video at 270 Mb/s to 8K ultra-high-definition (UHD) video at 23.76 Gb/s [5]–[9]. SDI ports are commonly available in professional video equipment such as cameras, recorders, vision mixers, desktop computers, monitors, among others. Despite widespread adoption of SDI, it offers limited flexibility to system designers, as cables need to be deployed between the equipment.

Alternatively, real-time wireless video links can be realized using optical wireless communication (OWC) [10]–[14]. In [10], Wei *et al.* implemented a real-time, multi-user optical wireless video transmission system using a micro-light-emitting diode (LED) bulb with two 50  $\mu\text{m}$  gallium nitride (GaN)  $\mu\text{LED}$  chips driven by a field-programmable gate array (FPGA) board based on quadrature amplitude modulation (QAM)-orthogonal frequency division multiplexing (OFDM). At the receiver side, each user is equipped with a photodiode (PD) and FPGA-based electronics to demodulate the QAM-OFDM signals. The setup achieved a combined data rate of 105.54 Mb/s over a 2 m free-space link with visual video fidelity and a measured end-to-end latency of 2 s. In [11], Li *et al.* experimentally demonstrated a free space optical (FSO) video transmission system using a laser source operating at 1550 nm and compressed sensing (CS). The system transmits compressed video frames at 20 frame/s via a simulated indoor atmospheric turbulence channel over a link distance of 2 m,

Hossein Kazemi (*corresponding author*), Isaac N. O. Osahon, Tiankuo Jiao, and Harald Haas are with the LiFi Research and Development Center (LRDC), Electrical Engineering Division, Department of Engineering, University of Cambridge, Cambridge CB3 0FA, United Kingdom.

David Butler is with the BBC Research & Development, London W12 7TQ, United Kingdom.

Nikolay Ledentsov Jr., Ilya Titkov, and Nikolay Ledentsov are with VI Systems GmbH (VIS), Berlin 10623, Germany.

achieving data rates of up to 3.125 Gb/s with a minimum bit error ratio (BER) of  $1.079 \times 10^{-11}$ , using an offline image reconstruction algorithm. In [12], Jeon *et al.* developed a real-time FSO system prototype to assess the feasibility of high-resolution video transmission over long distances for 6G networks. Their system integrates an FPGA-based software-defined radio (SDR) platform with a Mach–Zehnder modulator (MZM)-based channel emulator to mimic a 20 km terrestrial FSO link under realistic atmospheric conditions. The authors demonstrated real-time 4K UHD video transmission (i.e.,  $3840 \times 2160$  pixels transmitted at 60 frame/s) with a data rate of 35 Mb/s using pulse amplitude modulation (PAM)-4 modulation. By employing spatial selective filtering and a sampling-based pointing, acquisition, and tracking (PAT) technique to enhance signal quality, their prototype achieved a BER of about  $10^{-4}$  while maintaining reliable performance even under varying channel conditions. In [13], Al-Halafi *et al.* presented an underwater wireless optical communication (UWOC) system based on a directly modulated 520 nm laser diode (LD) at the transmitter and an avalanche photodiode (APD) at the receiver, supporting real-time video transmission over underwater channels up to 5 m. The system used QAM and phase shift keying (PSK) modulation schemes, achieving data rates up to 26.8 Mb/s with a BER as low as  $1.2 \times 10^{-9}$ , while transmitting a video resolution of  $640 \times 480$  pixels at 30 frame/s with an end-to-end latency under 1 s. Furthermore, in [14], Kong *et al.* proposed an underwater surveillance system, supporting real-time streaming of  $1920 \times 1080$  full HD (FHD) video at 30 frame/s. The underlying UWOC system employed a pair of high-power wide-beam LED transmitters and wide field of view (FOV) APD receivers without optical collimation or focusing elements in order to establish robust line-of-sight (LOS) links in dynamic underwater environments. The system achieved stable performance over 5 m in an outdoor pool with an end-to-end latency of about 250 ms, making it suitable for real-time underwater monitoring applications.

In this paper, we put forward a novel SDI over light fidelity (LiFi) system for real-time wireless video transmission with a submillisecond latency. We design a high-performance laser-based OWC system to implement direct modulation of the SDI output of a camera over the optical intensity of a vertical cavity surface emitting laser (VCSEL). The proposed system utilizes off-the-shelf SDI devices for real-time signal acquisition and conditioning, offering a low-cost and scalable solution for wireless connectivity between professional video equipment. To the best of our knowledge, this is the first experimental proof-of-concept for real-time transmission of high-definition (HD) video signals over optical wireless channels using SDI interfaces, supporting FHD and 4K UHD resolutions at data rates up to 6 Gb/s, while achieving an ultra-low latency of less than 35 ns for the end-to-end system.

The rest of the paper is organized as follows. In Section II, the design and implementation of the SDI over LiFi system are elaborated. In Section III, measurement results are presented and analyzed in terms of the real-time eye diagram and end-to-end latency. In Section IV, concluding remarks are given.

TABLE I  
SMPTE SDI STANDARDS [5]–[9]

Variant	Standard	Data Rate	Video Format
SD-SDI	ST 259	270 Mb/s	SD (480i @ 30 fps)
SD-SDI	ST 259	270 Mb/s	SD (576i @ 25 fps)
HD-SDI	ST 292	1.485 Gb/s	HD (720p @ 30 fps)
HD-SDI	ST 292	1.485 Gb/s	HD (1080i @ 25 fps)
3G-SDI	ST 424	2.97 Gb/s	FHD (1080p @ 50 fps)
3G-SDI	ST 424	2.97 Gb/s	FHD (1080p @ 60 fps)
6G-SDI	ST 2081	5.94 Gb/s	4K UHD (2160p @ 30 fps)
12G-SDI	ST 2082	11.88 Gb/s	4K UHD (2160p @ 60 fps)
24G-SDI	ST 2083	23.76 Gb/s	4K UHD (2160p @ 120 fps)
24G-SDI	ST 2083	23.76 Gb/s	8K UHD (4320p @ 30 fps)

fps denotes the frame rate unit [frame/s].

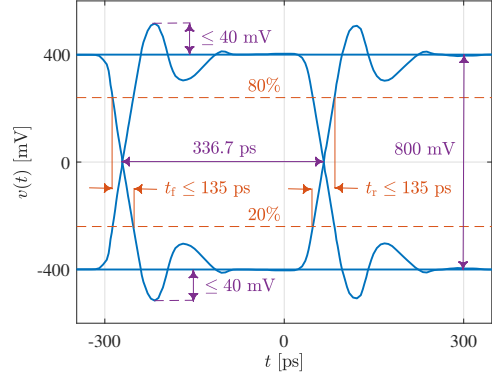


Fig. 1. 3G-SDI waveform measurement dimensions [6].

## II. SDI OVER LiFi SYSTEM DESIGN

In this section, we present the design of the proposed SDI-over-LiFi system. First, we provide an overview of the key specifications of the SDI signal interface with the objective of determining the dynamic range and bandwidth requirements for the system. Then, we present the experimental setup of the VCSEL-based optical wireless video transmission link. Table I provides the specifications of various SMPTE SDI standards in terms of their supported data rates and video formats [5]–[9].

### A. 3G-SDI Signal Interface

We use an HD camera for live video streaming. The camera is equipped with a 3G-SDI interface that generates a bit stream at a nominal bit rate of 3 Gb/s. According to the SMPTE ST 424 standard for 3 Gb/s serial interface [6], the 3G-SDI signal operates exactly at 2.97 Gb/s, and it has a rectangular pulse shape with a peak-to-peak amplitude of  $800 \text{ mV} \pm 10\%$  and a direct current (DC) offset of  $0.0 \text{ V} \pm 0.5 \text{ V}$ . Therefore, it is a bipolar signal that switches between  $\pm 400 \text{ mV}$  values. Fig. 1 shows the eye diagram specifications for the 3G-SDI waveform as defined by the SMPTE ST 424 standard [6]. The duration of one unit interval (UI) is 336.7 ps, corresponding to 2.97 Gb/s. The rise and fall times of the waveform, denoted by  $t_r$  and  $t_f$ , respectively, are determined between the 20% and 80% points of the peak-to-peak amplitude. In this case,  $t_r \leq 135 \text{ ps}$  and  $t_f \leq 135 \text{ ps}$  such that  $|t_r - t_f| \leq 50 \text{ ps}$ . The waveform exhibits an overshoot and an undershoot of up to 40 mV, equivalent to 10% of the peak amplitude.

In SDI video signals, binary information bits are encoded using a scrambled non-return-to-zero inverted (NRZI) channel

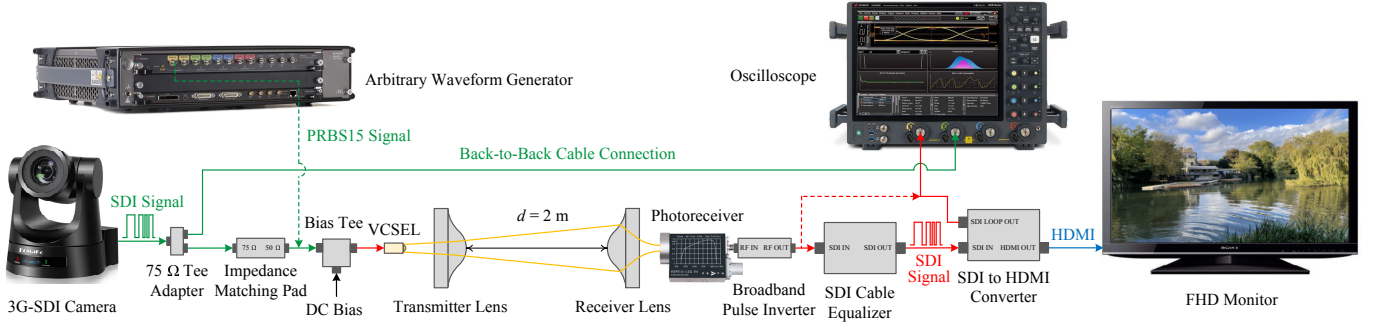


Fig. 3. Experimental setup for the proposed VCSEL-based SDI-over-LiFi link. The dashed green connection is used for emulating 3G-SDI signal transmission. The dashed red connection from the receiver output is used for latency measurements relative to the back-to-back signal from the camera.

coding scheme [6, Annex A]. Unlike non-return-to-zero (NRZ) encoding where binary data bits of ‘1’ and ‘0’ are represented by rectangular pulses of polarities  $A$  and  $-A$ , respectively, in NRZI encoding, transitions between the two amplitude levels occur only when a ‘1’ is transmitted, otherwise the amplitude level remains unchanged [15]. As a result, NRZI is a differential encoding scheme followed by NRZ signaling. A key advantage of differential encoding is the ability to detect errors in the event that some expected changes in the state of the signal are missing. This helps to maintain data synchronization even in scenarios where a long sequence of the same binary data is present, allowing the SDI signal to be properly synchronized at the receiver end. Moreover, according to the Nyquist-Shannon theorem, for baseband binary signal transmission at a bit rate of  $R_b$ , a system bandwidth of at least  $B = 0.5R_b$  is required [16]. Thus, the minimum bandwidth requirement for 3G-SDI signal is 1.5 GHz or 1.485 GHz to be precise. For safety margin, we may consider adding headroom for filtering and equalization tolerance, and design the front-end components of the system for a higher bandwidth of  $B = 0.7R_b$ , if needed. In this case, the minimum bandwidth requirement increases to 2 GHz.

### B. Experimental Setup

Fig. 2 shows the experimental setup of the proposed real-time SDI over LiFi system, streaming live video from an HD camera to a FHD monitor over an optical wireless link of length 2 m. Fig. 3 shows the complete experimental setup for the end-to-end system. The components used in the system setup are listed in Table II. The 3G-SDI signal is available at the SDI output port of the camera via a bayonet Neill–Concelman (BNC) type coaxial connector. This wideband analog signal is directly modulated on the intensity of a 940 nm single-mode (SM) VCSEL at the transmitter by using a bias tee (BT). The VCSEL was developed, fabricated and packaged by Vertically Integrated Systems (VIS) GmbH, and underwent wafer-level testing prior to full characterization for high-speed optical communications [17]. It has a multi-aperture (MA) structure consisting of four VCSELs that are arranged in a compact  $2 \times 2$  mini-array configuration with a pitch of  $< 15$  nm. These four VCSELs are driven by a common pair of contacts and their outputs are strongly coupled such that they effectively operate as a single VCSEL [17]. In

TABLE II  
SYSTEM COMPONENTS

Component	Manufacturer	Model	Bandwidth/Rate
Camera	FoMaKo	PTZ 3G-SDI	3 Gb/s
RFS	Telegartner	75 Ω Tee Adapter	4 GHz
BT	Mini-Circuits	ZX85-12G-S+	12 GHz
ACL	Thorlabs	ACL7560U-B	—
PR	FEMTO	HSPR-X-I-2G-IN	2 GHz
CEQ	Extron	12G HD-SDI 101	12 Gb/s
SHC	Blackmagic	12G	12 Gb/s
AWG	Keysight	M8195A	6 GHz, 16 GSa/s
OSC	Keysight	UXR0104B	10 GHz, 128 Ga/s

RFS: RF Splitter; PR: Photoreceiver; SHC: SDI to HDMI Converter

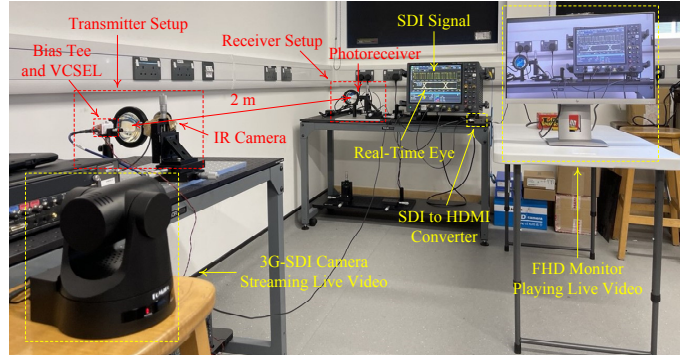


Fig. 2. Live video streaming from a 3G-SDI camera to a FHD monitor via the VCSEL-based SDI-over-LiFi link over a 2 m distance.

this way, the output power increases while preserving the SM emission spectrum. The MA VCSEL exhibits a near-Gaussian beam profile with a far field (FF) full-width at half-maximum (FWHM) divergence angle of  $18^\circ$ , a peak optical power of 14 mW, and a 3-dB modulation bandwidth of 18 GHz. It also offers a linear input dynamic range between a forward threshold current of 2 mA and a roll-over current of 30 mA.

In optical intensity modulation and direct detection (IM/DD) systems, the modulating signal is non-negative and real-valued. In particular, in laser-based optical IM/DD systems using non-return-to-zero on-off keying (NRZ-OOK) modulation scheme, a DC offset is added to the bipolar NRZ signal. To this end, the laser is typically biased slightly below its turn-on threshold, allowing it to produce a continuous optical signal during the transmission period for a data bit of ‘1’ and to be effectively turned off for a data bit of ‘0’ [18]. This is a viable approach as long as the laser source can be switched on and off at a

speed matching the bit rate of the NRZ pulse. Although the modulation bandwidth of the VCSEL is larger than the bit rate of the 3G-SDI signal, we opt for a sufficiently high DC bias level to ensure operation within the linear dynamic range of the VCSEL to further improve the laser response time and avoid nonlinear distortion effects. Based on the light-current-voltage (LIV) characteristics of the VCSEL, we choose a DC operating point in the middle of the linear dynamic range by setting  $V_{DC} = 2.4$  V and  $I_{DC} = 8.42$  mA. Consequently, the VCSEL is never turned off and a maximally linear dynamic range is provided for the SDI signal swing. The BT has a wideband frequency range of 200 kHz to 12 GHz with a low insertion loss (IL) of  $IL < 1$  dB over the signal bandwidth. The SDI output of the camera is connected to the BT using a 12G-SDI cable, which supports bit rates up to 12 Gb/s. SDI cables are 75  $\Omega$  wideband coaxial cables with BNC connectors<sup>1</sup>. Since the BT has an input impedance of 50  $\Omega$ , we use an impedance matching pad to convert 75  $\Omega$  to 50  $\Omega$  before feeding the SDI signal into the BT, as shown in Fig. 3. The biased SDI signal is then fed into the VCSEL using a 26 GHz radio frequency (RF) coaxial cable with  $IL < 1$  dB over the desired bandwidth. To achieve beam collimation at the transmitter, an aspheric condenser lens (ACL) is positioned in front of the VCSEL. This ACL has a diameter of 50 mm, a focal length of 40 mm, a numerical aperture (NA) of 0.6, and is equipped with an anti-reflective coating (ARC) for 650–1050 nm wavelength range.

At the receiver side, located 2 m away from the transmitter, the incident light beam is collected by an ACL, identical to the transmitter lens, and is focused on a high-speed photodetector. Specifically, we employ a wideband positive-intrinsic-negative (PIN) photoreceiver with lower and upper  $-3$  dB cut-off frequencies of 10 kHz and 2 GHz, respectively. It consists of an InGaAs PD with an active area of 100  $\mu\text{m}$ , followed by an integrated low-noise transimpedance amplifier (TIA). The PD operates over a spectral range of 900–1700 nm with a maximum responsivity of 0.95 A/W at 1550 nm, and it has a responsivity of about 0.5 A/W at the VCSEL wavelength (i.e., 940 nm). The TIA is an inverting amplifier that provides a transimpedance gain of  $5.0 \times 10^3$  V/A, resulting in a conversion gain of  $2.5 \times 10^3$  V/W at 940 nm. The photoreceiver generates an alternating current (AC)-coupled output voltage with a maximum peak-to-peak amplitude of 2.0 V. The output signal has an inverted polarity with respect to the input SDI signal. To revert back to the original polarity, we employ a broadband pulse inverter (BPI) at the receiver output, as shown in Fig. 3. The BPI is a two-port device that introduces a phase shift of  $180^\circ$  relative to its input signal while maintaining a flat group delay over a broadband frequency range of 1 MHz to 40 GHz. It has an IL of about 2 dB over the SDI signal bandwidth. The detected signal is subsequently fed into an SDI cable equalizer (CEQ) using a 12G-SDI cable. The CEQ automatically adapts to SMPTE serial digital video standards for SDI signals up to a 12G-SDI data rate. It compensates for cable attenuation of up to  $-30$  dB over distances of up to 240 m, specifically for HD-SDI signals. It also reshapes and restores signal timing using

an embedded reclocking repeater, eliminating high-frequency jitter<sup>2</sup>. We employ an SDI to HDMI converter to convert the received SDI video stream to an HDMI signal and cast it on the FHD monitor. This converter also has an SDI loop out, providing a replica of its input SDI signal, which is connected to the oscilloscope (OSC) for real-time eye diagram measurements, as shown in Fig. 3. The OSC performs analog-to-digital conversion (ADC) at a sampling rate of 32 GSa/s to improve measurement accuracy and capture fine details of the received 3G-SDI signal.

Before connecting the camera and monitor, proper operation of the SDI over LiFi system should be verified. To this end, we generate a pseudorandom binary sequence (PRBS) of length  $2^{15} - 1$  bits in MATLAB. Then, by using an arbitrary waveform generator (AWG), we turn the resulting PRBS15 bit stream into an NRZ encoded waveform with the same bit rate as the 3G-SDI signal based on binary phase-shift keying (BPSK) modulation with rectangular pulse shaping. After DC biasing, the PRBS15 NRZ signal is sent over the VCSEL-based optical wireless link in order to emulate 3G-SDI signal transmission. This is indicated by a dashed green connection in Fig. 3. The real-time eye diagram of the equalized signal at the receiver yields an accurate estimate of the system performance during 3G-SDI signal transmission. Eye diagram measurements are discussed in the following section.

### III. MEASUREMENT RESULTS

We present experimental results for the real-time eye pattern and end-to-end latency measurements. First, let us introduce an important quality metric used for performance analysis.

#### A. Link Quality Metric

A widely used performance metric for optical signals is the  $Q$ -factor [20]. For an IM/DD optical communication system based on NRZ on-off keying (OOK) modulation, the  $Q$ -factor is defined as [20]:

$$Q = \frac{V_s}{\sigma_n}, \quad (1)$$

where  $V_s$  is the amplitude of the received signal and  $\sigma_n$  is the standard deviation of noise at the receiver. The corresponding signal-to-noise ratio (SNR) and BER are given by [20]:

$$\text{SNR} = Q^2, \quad (2)$$

$$\text{BER} = \frac{1}{2} \text{erfc} \left( \frac{Q}{\sqrt{2}} \right), \quad (3)$$

where  $\text{erfc}$  denotes the complementary error function given by  $\text{erfc}(z) = \frac{2}{\sqrt{\pi}} \int_z^\infty e^{-u^2} du$ .

Since SDI is a point-to-point interface, the feasibility of an SDI link to operate reliably at a given data rate is determined primarily by the link distance (i.e., cable length). In practice, the BER performance rapidly deteriorates beyond a critical cable length known as the crash knee [4]. This critical distance

<sup>1</sup>Compared to the characteristic impedance of 50  $\Omega$ , commonly used in RF test and measurement equipment, 75  $\Omega$  coaxial cables with BNC connectors used for analog video transmission exhibit lower attenuation [19].

<sup>2</sup>The reclocking repeater does not decode, descramble, or deserialize the data stream. Rather, it equalizes, slices, and reclocks the input signal using a phase-locked loop (PLL) to reject jitter and noise, thereby recovering a clean binary signal, which can then be forwarded to an SDI line driver [4].





(a) At 2.97 Gb/s for 3G-SDI



(b) At 5.94 Gb/s for 6G-SDI

Fig. 4. Real-time eye patterns for received PRBS15 NRZ test signals.

is identified at the point where at most 1 bit error occurs in a given period of time. In particular, HD-SDI links with a target performance of 1 bit error per second and 1 bit error per hour, corresponding to BER thresholds of  $4.7 \times 10^{-9}$  and  $1.3 \times 10^{-12}$ , can reach distances of up to 188 m and 182 m, respectively, based on the phase alternating line (PAL) TV broadcasting system [4]. From (2) and (3), these BER values translate into a minimum  $Q$ -factor of 5.7 and 7, equivalent to a minimum required SNR of 15.2 dB and 16.9 dB, respectively.

### B. Real-Time Eye Pattern

The eye pattern is an effective tool for evaluating the quality of signals in digital communications. An eye pattern is formed by the synchronized superposition of all possible realizations of the signal of interest when observed within a given signaling interval [16]. The vertical and horizontal eye openings are key characteristics of the eye diagram. The vertical eye opening reflects the noise margin of the signal and is indicative of the SNR, while the horizontal eye opening corresponds to the timing margin and provides insight into the extent of timing jitter and inter-symbol interference (ISI) [16].

Fig. 4 shows the real-time eye patterns on the OSC for received PRBS15 NRZ signals at data rates of 2.97 Gb/s and 5.94 Gb/s to emulate 3G-SDI and 6G-SDI video transmissions, respectively, as indicated in Table I. It can be seen that the eye diagrams in both cases are wide-open both horizontally and vertically, demonstrating the excellent performance of the SDI over LiFi system. For the PRBS15 NRZ test link at 2.97 Gb/s, as shown in Fig. 4(a), a  $Q$ -factor of 27.42 is achieved, which



Fig. 5. Real-time eye pattern for the received 3G-SDI signal from the camera.

translate into an SNR value of 28.76 dB. When the data rate is doubled, as shown in Fig. 4(b), the  $Q$ -factor reduces to 14.22, equivalent to an SNR value of 23.06 dB. However, this  $Q$ -factor is more than twice greater than the  $Q$ -factor threshold of 7 required to keep the BER level below  $1.3 \times 10^{-12}$ . This evinces that the system already supports the 6G-SDI signal transmission with almost error-free performance.

Fig. 5 shows the real-time eye diagram on the OSC for the received 3G-SDI signal from the camera. It can be observed that the  $Q$ -factor is improved to 32.50 compared to the corresponding PRBS15 NRZ test link, as shown in Fig. 4(a), resulting in an SNR value of 30.24 dB. This is due to the fact the CEQ has optimum performance for standard SDI video signals. With this SNR level, the SDI over LiFi link operates at an extremely low BER based on (3).

### C. End-to-End Latency

The system setup used for end-to-end latency measurements is shown in Fig. 3. A replica of the input SDI signal is used as the reference signal. To this end, a back-to-back connection is extended from the camera to the OSC using a 75  $\Omega$  RF tee adapter (i.e., splitter) at the 3G-SDI output of the camera. The tee adapter equally divides the RF power between its two output ports<sup>3</sup> over a frequency range of DC to 4 GHz. For time delay estimation, we apply the cross-correlation technique using a large number of signal samples [21]. Let  $x(t)$  and  $y(t)$ , respectively, denote the back-to-back signal and the received signal before the CEQ, as shown in Fig. 3. For these two real signals, the sample cross-correlation function is computed by [21]:

$$\begin{aligned} \hat{R}_{xy}(\tau) &= \frac{1}{N} \sum_{k=1}^N x(t)y(t+\tau)|_{t=kT}, \\ &= \frac{1}{N} \sum_{k=1}^N x(kT)y(kT+\tau), \end{aligned} \quad (4)$$

where  $N$  is the total number of samples, and  $T$  is the sampling period, and  $W = (N - 1)T$  is the duration of the estimation window. The time delay between the two signals, denoted by  $\tau_d$ , is determined by the point in time where the direct

<sup>3</sup> Although this leads to a 3 dB loss for each signal path and the SDI signal that reaches the VCSEL is slightly attenuated, the peak-to-peak amplitude of the signal is still sufficient to ensure a high SNR, as reported in Section III-B.

correlator in (4) is maximized, indicating the relative time shift at which they align best with each other in terms of similarity. This can be expressed as [21]:

$$\tau_d = \arg \max_{\tau} \hat{R}_{xy}(\tau). \quad (5)$$

Note that this is the relative delay between the output signal and the reference signal through the back-to-back connection. Let  $\tau_{ow}$  and  $\tau_{bb}$  denote the end-to-end latency of the SDI over optical wireless link and the delay caused by the back-to-back cable, respectively. We have  $\tau_d = \tau_{ow} - \tau_{bb}$ , which leads to:

$$\tau_{ow} = \tau_d + \tau_{bb}. \quad (6)$$

Fig. 6 shows the time delay estimation based on maximizing the cross-correlation between the input and output SDI signals. With the OSC operating at 32 GSa/s, for each signal, a total of  $N = 32001$  samples are obtained over an interval of length  $W = 1000$  ns to compute the cross-correlation function, as plotted in Fig. 6(a), resulting in  $\tau_d = 8.56$  ns. To verify this value, a time shift of  $t + \tau_d$  is introduced to the output signal to be compared with the input signal. For clarity, the results are plotted in a 40 ns interval, as shown Fig. 6(b), confirming that the two signals are in perfect agreement when the computed time delay is applied. The delay due to the back-to-back cable is directly measured using a broadband performance network analyzer (PNA) based on the the forward voltage gain (i.e.,  $S_{21}$ ) of the cable. It is found to be  $\tau_{bb} = 12.18$  ns across the operating bandwidth of the cable (i.e.,  $> 6$  GHz). Based on (6), we obtain:

$$\tau_{ow} = 8.56 + 12.18 = 20.74 \text{ ns}. \quad (7)$$

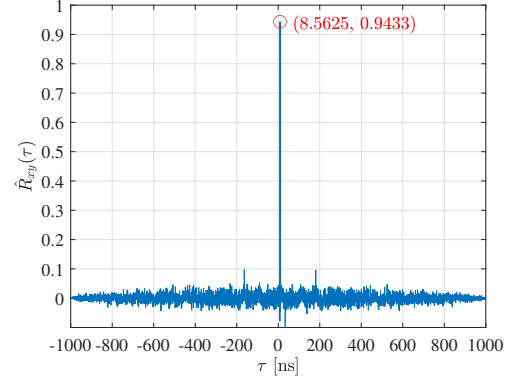
The CEQ has a flat latency of 14 ns for SDI video equalization and reclocking. Taking into account this delay component, the end-to-end latency of the SDI over LiFi system is obtained as:

$$\tau_{SDI} = 20.74 + 14 = 34.74 \text{ ns}. \quad (8)$$

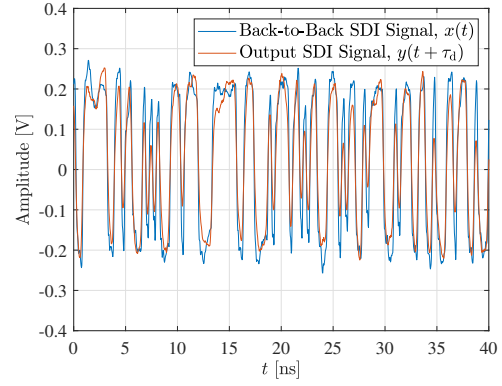
We note that the SDI to HDMI converter introduces a delay on the order of a few scan lines of video during signal conversion, which is typically less than one video frame. According to the SMPTE ST 424 standard [6], the direct mapping of an FHD video stream with a 1080p resolution (i.e.,  $1920 \times 1080$ ) into an SDI data stream using 3G-SDI Level A format requires a total line count of 1125 per frame. For a frame rate of 60 frame/s, the frame duration is  $1/60 \approx 16.67$  ms, and thus the line duration is  $16.67/1125 \approx 14.81$   $\mu$ s. Consequently, the delay associated with the SDI to HDMI conversion for 5 to 10 lines is estimated as 74 to 148  $\mu$ s.

#### IV. CONCLUSIONS

In this paper, we have demonstrated real-time and error-free transmission of HD video signals over a VCSEL-based optical wireless link using a high-performance SDI over LiFi system. Based on a 3G-SDI camera, we have experimentally validated the real-time transmission of a live video stream with a 1080p FHD resolution at 60 frame/s and a data rate of 2.97 Gb/s over a link distance of 2 m with a measured end-to-end latency of  $< 35$  ns, while achieving an eye diagram  $Q$ -factor of  $> 32$ , which corresponds to an SNR of  $> 30$  dB. Based on a PRBS15



(a) Normalized cross-correlation function



(b)  $x(t)$  vs.  $y(t + \tau_d)$  for  $\tau_d = 8.56$  ns

Fig. 6. Estimating the time delay between the input SDI signal,  $x(t)$ , and the output SDI signal,  $y(t)$ , based on their cross-correlation,  $\hat{R}_{xy}(\tau)$ .

bit stream to emulate 6G-SDI signal transmission, the SDI over LiFi system proves effective in real-time streaming of 4K UHD video signals with a resolution of 2160p at 30 frame/s and a data rate of 5.94 Gb/s, with a  $Q$ -factor of  $> 14$ , which is more than twice the  $Q$ -factor threshold of 7 for a BER performance of  $1.3 \times 10^{-12}$ . Considering the 18 GHz modulation bandwidth of the VCSEL, the 2 GHz bandwidth of the receiver currently limits the performance of the end-to-end system. This system can potentially support the real-time transmission of 12G-SDI or even 24G-SDI signals based on a single VCSEL, for higher video resolutions up to 8K UHD, provided that a receiver with sufficiently high bandwidth is used. Scaling the system design to support higher video resolutions and/or frame rates will be addressed in our future works.

#### ACKNOWLEDGEMENT

This work was financially supported by the Engineering and Physical Sciences Research Council (EPSRC) under grant EP/Y037243/1 ‘Platform Driving The Ultimate Connectivity (TITAN)’. The authors thank Srinjoy Dey for his valuable support in ensuring the successful demonstration of the proposed system during the Connected Futures Festival and the Cambridge 6G Symposium.

## REFERENCES

- [1] A. Hazra, A. Munusamy, M. Adhikari, L. K. Awasthi, and V. P., "6G-Enabled Ultra-Reliable Low Latency Communication for Industry 5.0: Challenges and Future Directions," *IEEE Commun. Stand. Mag.*, vol. 8, no. 2, pp. 36–42, 2024.
- [2] C.-X. Wang *et al.*, "On the Road to 6G: Visions, Requirements, Key Technologies, and Testbeds," *IEEE Commun. Surveys Tuts.*, vol. 25, no. 2, pp. 905–974, 2023.
- [3] C. Poole, "Low-Latency Streaming Trial on BBC iPlayer," *BBC Research & Development*, Jun. 2025. [Online]. Available: <https://www.bbc.co.uk/rd/articles/2025-06-low-latency-streaming-iplayer>
- [4] J. Watkinson and F. Rumsey, *Digital Interface Handbook*, 3rd ed. Elsevier Focal Press, 2004.
- [5] *SMPTE ST 259:2008 - for Television – Standard Definition Television (SDTV) – Serial Digital Interface*, Society of Motion Picture and Television Engineers Std., Jan. 2008.
- [6] *SMPTE ST 424:2012 - 3 Gb/s Signal/Data Serial Interface*, Society of Motion Picture and Television Engineers Std., Dec. 2013.
- [7] *SMPTE ST 2081-1:2015 – 6 Gb/s Signal/Data Serial Interface*, Society of Motion Picture and Television Engineers Std., May 2015.
- [8] *SMPTE ST 2082-1:2015 – 12 Gb/s Signal/Data Serial Interface*, Society of Motion Picture and Television Engineers Std., May 2015.
- [9] *SMPTE ST 2083:2020 – 24 Gb/s Signal/Data Serial Interface*, Society of Motion Picture and Television Engineers Std., Jan. 2020.
- [10] Z. Wei *et al.*, "Real-Time Multi-User Video Optical Wireless Transmission Based on a Parallel Micro-LEDs Bulb," *IEEE Photon. J.*, vol. 13, no. 3, pp. 1–11, Jun. 2021.
- [11] J. Li *et al.*, "Experimental demonstration of a free space optical wireless video transmission system based on image compression sensing algorithm," *Optica Opt. Express*, vol. 31, no. 25, pp. 41 479–41 495, Dec. 2023.
- [12] H.-B. Jeon *et al.*, "Free-Space Optical Communications for 6G Wireless Networks: Challenges, Opportunities, and Prototype Validation," *IEEE Commun. Mag.*, vol. 61, no. 4, pp. 116–121, Apr. 2023.
- [13] A. Al-Halafi *et al.*, "Real-Time Video Transmission Over Different Underwater Wireless Optical Channels Using a Directly Modulated 520 nm Laser Diode," *IEEE/Optica J. Opt. Commun. Netw.*, vol. 9, no. 10, pp. 826–832, Oct. 2017.
- [14] M. Kong, Y. Guo, O. Alkhazragi, M. Sait, C. H. Kang, T. K. Ng, and B. S. Ooi, "Real-Time Optical-Wireless Video Surveillance System for High Visual-Fidelity Underwater Monitoring," *IEEE Photon. J.*, vol. 14, no. 2, pp. 1–9, Apr. 2022.
- [15] J. G. Proakis and M. Salehi, *Digital Communications*, 5th ed. McGraw-Hill, 2008.
- [16] S. Haykin and M. Moher, *Communication Systems*, 5th ed. Wiley, 2009.
- [17] N. Ledentsov Jr. *et al.*, "Advances in design and application of compact VCSEL arrays: from multicore fiber to optical wireless and beyond," in *Vertical-Cavity Surface-Emitting Lasers XXVI*, vol. 12020, International Society for Optics and Photonics. SPIE, 2022, p. 1202008.
- [18] G. P. Agrawal, *Lightwave Technology: Telecommunication Systems*. Wiley, 2005.
- [19] W. Fischer, *Digital Video and Audio Broadcasting Technology: A Practical Engineering Guide*, 4th ed. Springer, 2020.
- [20] W. Freude, R. Schmogrow, B. Nebendahl, M. Winter, A. Josten, D. Hillerkuss, S. Koenig, J. Meyer, M. Dreschmann, M. Huebner, C. Koos, J. Becker, and J. Leuthold, "Quality Metrics for Optical Signals: Eye Diagram, Q-factor, OSNR, EVM and BER," in *Proc. 14th International Conference on Transparent Optical Networks (ICTON)*, Jul. 2012, pp. 1–4.
- [21] G. Jacovitti and G. Scarano, "Discrete Time Techniques for Time Delay Estimation," *IEEE Trans. Signal Process.*, vol. 41, no. 2, pp. 525–533, 1993.



**Hossein Kazemi** (Member, IEEE) received the Ph.D. degree in Electrical Engineering from The University of Edinburgh, U.K., in 2019. He also received the M.Sc. degree in Electrical Engineering (Microelectronic Circuits) from Sharif University of Technology, Tehran, Iran, in 2011, and the M.Sc. degree (Hons.) in Electrical Engineering (Wireless Communications) from Ozyegin University, Istanbul, Turkey, in 2014. He is a Postdoctoral Research Associate at the LiFi Research and Development Center, University of Cambridge, U.K. Dr Kazemi was the recipient of the Best Paper Award for the 2022 IEEE Global Communications Conference (GLOBECOM). His current research interests include the design, analysis and optimization of ultra-high-speed optical wireless communication systems for 6G and beyond networks.



**Isaac N. O. Osahon** (Member, IEEE) received the B.Eng. degree in Electrical and Electronic Engineering (first class hon.) from Covenant University, Ota, Nigeria, in 2012, the M.Sc. degree in Internet Engineering from the University College London, London, in 2015, and the Ph.D. degree at the Institute of Digital Communications, The University of Edinburgh, in 2020. He has worked as a researcher on digital signal processing for optical fiber and wireless communication systems in notable U.K. universities. He is a Postdoctoral Research Associate

at the LiFi Research and Development Center, University of Cambridge, U.K. His current research interests include optical communications, advanced modulation schemes, artificial neural networks, digital equalization techniques, visible light positioning and physical layer security.



**Tiankuo Jiao** received the B.Eng. degree in Electrical and Electronic Engineering with First Class Honors from the University of Liverpool, U.K., in 2023. He subsequently earned an M.Res. degree in Photonic and Electronic Systems from the University of Cambridge, U.K., in 2024. He is currently pursuing a Ph.D. at the LiFi Research and Development Center (LRDC), University of Cambridge, where his research focuses on the design and implementation of coherent optical wireless communication (OWC) systems and the development of advanced digital

signal processing (DSP) algorithms for next-generation light fidelity (LiFi) connectivity.



**David Butler** received the M.Eng. degree in Electrical and Electronic Engineering from the University of Bath, U.K., in 1991. He is currently a Senior R&D Engineer at BBC Research and Development, where he has over 25 years of experience in the communications and broadcasting industry. His work encompasses the design, prototyping, and deployment of end-to-end systems, with particular emphasis on analog and radio frequency (RF) technologies. He has contributed extensively to the development of broadcast infrastructure and has played a key role in

advancing technical innovations within the BBC. His areas of specialization include RF systems, signal processing, and system integration across the full product life cycle.





**Nikolay Ledentsov Jr.** received his B.Sc. and M.Sc. degrees from the Technical University of Berlin, Germany, in 2012 and 2014, respectively, where his research focused on the growth and characterization of Indium Aluminum Gallium Nitride (InAlGaN) green and ultraviolet (UV) light emitting diodes (LEDs). He completed his Ph.D. at the Technical University of Warsaw, Poland, in 2023, focusing on high-speed data transmission with infrared (IR) vertical-cavity surface-emitting lasers (VCSELs). He was a Senior Engineer at VI Systems GmbH, where

he was responsible for the research and development of VCSELs for high-speed optical links, and manufacturing and characterization of light emitters and photodiodes. He is currently head of the characterization and VCSEL development at EPIGAP OSA Photonics GmbH.



**Harald Haas** (Fellow, IEEE) received his Ph.D. from The University of Edinburgh, U.K., in 2001. He is the Van Eck Chair of Engineering at the University of Cambridge and the founder of pureLiFi Ltd., where he also serves as the Chief Scientific Officer (CSO). His recent research interests focus on photonics, communication theory and signal processing for optical wireless communication systems. Since 2017, he has been recognised as a highly cited researcher by Clarivate/Web of Science. He has delivered two TED talks and one TEDx talk. In

2016, he received the Outstanding Achievement Award from the International Solid State Lighting Alliance. He was awarded the Royal Society Wolfson Research Merit Award in 2017, the IEEE Vehicular Technology Society James Evans Avant Garde Award in 2019, and the Enginuity: The Connect Places Innovation Award in 2021. In 2022, he received the Humboldt Research Award for his research contributions. He is a Fellow of the Royal Academy of Engineering (RAEng), the Royal Society of Edinburgh (RSE), and the Institution of Engineering and Technology (IET). In 2023, he was shortlisted for the European Inventor Award.



**Ilya Titkov** received his Ph.D. degree in Semiconductor Manufacturing Technology from Peter the Great St. Petersburg Polytechnic University, Saint Petersburg, Russia, in 2000. From 2002 to 2009, he worked as a researcher at the Ioffe Institute's Laboratory of Semiconductor Devices Physics in Saint Petersburg, Russia, where he focused on semiconductor material physics and oxide-based device structures. Since 2014, he has held a research position at the Aston Institute of Photonic Technologies, Aston University, Birmingham, U.K., contributing to

LED efficiency analysis and photonic device development. He currently serves as R&D Manager and Senior Researcher at VI Systems GmbH, specializing in advanced characterization methods and failure analysis for high-speed VCSEL technologies and optoelectronic devices.



**Nikolay Ledentsov** (Senior Member, IEEE) received the Diploma in electrical engineer from the Electrical Engineering Institute, Leningrad, Russia, in 1982, the Ph.D. (Cand. Sci.) and Dr. Sci. (Habil.) degrees in physics and mathematics from A. F. Ioffe Institute, Leningrad/Saint Petersburg, Russia, in 1987 and 1994, respectively. Since 1994, he has been a Professor of electrical engineering and, since 2005, a certified Professor of physics and mathematics with Ioffe Institute. During 1996–2007, he was a Professor with the Technical University of

Berlin, Berlin, Germany. He has authored or coauthored more than 900 papers in technical journals and conference proceedings and 38 patent families. His Hirsch factor is 83. His current research interests include physics and technology of semiconductor nanostructures and design and technology of advanced optoelectronic devices. He is a Fellow of the Institute of Physics and a Member of the Russian Academy of Sciences. He was the recipient of the Young Scientist Award from the International Symposium on Compound Semiconductors in 1996 for outstanding contributions to the development of physics and MBE growth of InGaAs/GaAs quantum dots structures and quantum dot lasers, State Prize of Russia for Science and Technology in 2001, Prize of the Berlin Brandenburg Academy of Sciences in 2002, and other awards and recognitions. During 1995–1996, he was the recipient of Alexander von Humboldt Fellowship. Since 2006, he has been the Chief Executive Officer of VI Systems GmbH.